International Information and Engineering Technology Association
Advancing the World of Information and Engineering

Mathematical Modelling of Engineering Problems
Vol. 11, No. 9, September, 2024, pp. 2447-2462
Journal homepage: http://iieta.org/journals/mmep

Free Vibration Analysis of a Simply Supported Axial Functionally Graded Beam Using the Rayleigh Method

Jaafar Mohammed Yadeem[1], Kadhum Jassem Wadia[2], Husam Jawad Abdulsamad[3*], Luay S. Alansari[3]

[1] Ministry of Education, General Directorate of Vocational Education, Baghdad 10001, Iraq
[2] Technical Instructors Training Institute, Middle Technical University, Baghdad 10001, Iraq
[3] Department of Mechanical Engineering, College of Engineering, University of Kufa, Najaf 54001, Iraq

Corresponding Author Email: husamj.alhamad@uokufa.edu.iq

https://doi.org/10.18280/mmep.110917

Received: 11 June 2023
Revised: 13 November 2023
Accepted: 30 November 2023
Available online: 29 September 2024

Keywords:
power-law index, modulus ratio, density ratio, axial functionally graded material, natural frequency, mode shape

ABSTRACT

This study aims to make investigation for the free vibration problem of simply supported axial-FGB by applying the Rayleigh method. The model of (power law) is adopted to describe the change in physical mechanical and properties through the axial direction. The computer program is built in this work. The accuracy of Rayleigh method is checked by comparison of the results of Rayleigh method with the results available in literatures and a very good accuracy was found. The combined effects of power-law index, modulus-ratio and density-ratio on the fundamental frequency and mode shapes of axial-FGBs are investigated. The results explain that the non-dimensional frequency parameter at any modulus-ratio is approximately constant when the power-law index increases. When the power-law index is smaller than (1), the effect of modulus-ratio is greater than the effect of density-ratio. While the effect of modulus-ratio is smaller than the effect of density-ratio when the power-law index is greater than (1). Also, when density-ratio equals (1), the dimensionless deflection (or amplitude) increases with reducing of power-law index (β). When the modulus-ratio is smaller than (1), the dimensionless deflection increases with increasing the power-law index (β). From results, the Rayleigh method is able to calculate the natural frequency and mode shape of simply supported axial-FGM beam.

1. INTRODUCTION

In the last twenty years, a new kind of composite materials has been widely used in several engineering applications (such as space crafts, vehicles, aircrafts, electronics, biomedical field and defense and military industries) because of their developed properties, and this kind of composite is called "functionally graded material (FGM)" [1]. FGMs, like traditional composite materials, consist of a combination of two separated components which graded along one, two or three directions and the one dimension FGM is divided into two types thickness and axial-FGM [2-4]. This gradation in material properties of FGMs leads to reduce the effects residual stresses, shear stresses, thermal stresses and stress concentrations between the components [1, 5-9].

Due to the several advantages of FGMs, many engineering applications used these materials into several structures such as beams, plates and shells. In the last few years, a lot of studies were accomplished for understanding the impacts of FGMs on the static and dynamic behaviors of beams, plates and shells. The growing use of FG beams as structural components in numerous areas has necessitated the study of their dynamic behavior and particular vibration characteristics (natural frequency and mode shape) [10, 11].

In general, it is difficult to find an exact solution of the vibration phenomena of axial-FG beam due to the complexity of the governing differential equation. Therefore, various methods or techniques (such as finite element method, finite different method, power series technique, Homogenization technique, Semi-analytical technique, Rayleigh method, etc.) have been applied to solve and study the vibration phenomena of axial-FG beam. In 2004, the semi-inverse method was applied by Elishakoff and Guede to solve a free vibration problem of a large class of FG beam [12]. Çalım [13] studied the dynamic problem of nonuniform composite beams using an efficient method of analysis in the Laplace domain. Huang and Li [14] used a combination of differential equation with variable coefficients and the boundary conditions to find "Fredholm integral equation". They salved "Fredholm integral equation" to estimate the natural frequencies and buckling loads of axial-FG beams.

Alshorbagy et al. [15] used a basic power law model to characterize the materials distribution in length direction to investigate the free vibration problem of axial-FG beams. They applied the finite element method by developing new element (element has two nodes and six-degree of freedom) basing on Euler-Bernoulli beam theory. Also, the finite element method was used by Shahba et al. to investigate the free vibration behavior of tapered axial-FG beam basing on Euler-Bernoulli and Timoshenko beam theories [16, 17].

Shahba and Rajasekaran [18] applied the “differential transform element method” to calculate the natural frequency of tapered axial-FG beam basing on Euler-Bernoulli theory. For varying cross sections, the vibration behaviors of axial-FG beam with different supporting types were investigated by Hein and Feklistova [19] using “Haar wavelet series”. Huang et al. [20] considered Timoshenko theory to develop a new approach by presenting an auxiliary function. to study the effect of non-uniformity parameter of cross section on the vibration analysis of axial-FG beams. Akgöz and Civalek [21] used both modified couple stress and Bernoulli-Euler beam theory to estimate the natural frequency of axial-FG beams with linear variation of cross section. Li et al. [22] adopted exponential model to describe variation of material properties and cross-section area parameter along the length of FG beams by applying Euler-Bernoulli theory and Timoshenko beam theory [23]. For uniform axial-FG beam, Sarkar and Ganguli based Timoshenko theory to investigate the effect of supporting types on the natural frequency [24].

Garijo [25] applied "collocation technique" and "Bernstein polynomials" to study the impact of varying cross section of axial FG beam on the natural frequency. Basing on " Chebyshev polynomial " theory, the free vibration of non-prismatic axial-FG was investigated by Zhao et al. [26] and Liu et al. [27] used the “spline finite point method” to study the same cases. Xie et al. [28] investigated the free vibration behavior of beams with varying in densities, moduli of elasticity and cross section in axial direction using decomposition technique, integrated polynomials and the spectral collocation approach. Kukla and Rychlewska [29] investigated the natural frequency of axial-FG beam by replacing functions characterizing FG beams with piecewise "exponential functions". The natural frequency of non-prismatic axial-FG beam was estimated by Huang and Rong [30]. They based on integral technique and polynomial expansion as well as Euler-Bernoulli beam theory to propose a new simple approach in their analysis. Cao et al. [31] studied analytically the free vibration analysis of axial FG beam using “the perturbation theory and Meijer G-Function" and Euler-Bernoulli beam theory. They found that “the new two analytical methods are simple and efficient and can be used to conveniently analyze free vibration of AFG beam”. Fogang [32] applied the finite difference method to analyze the vibration problems of non-uniform axial-FG beam basing on Timoshenko theory. He assumed that the material and geometry parameters (density, elastic and shear moduli, moment of inertia and cross section area) changed along the axial direction. Kılıç and Özdemir [33] investigated the buckling and vibration behaviors of axial-FG beam using finite element technique and basing on the classical and the first order shear deformation theories. They investigated the impact of rotational speed, radius of hub, material properties, material distribution parameter as well as supporting type. Selmi [34] estimated the mode shapes and natural frequencies of axial-FG beam by applying “Differential Transformation Method" and compared the results that obtained by the "Differential Transformation Method" with that obtained by finite element method. He studied the impact of material distribution parameter, density ratio and modulus ratio.

In this study, Rayleigh method was modified to investigate the free vibration problem of simply supported axial-FG beam. The varying in physical and mechanical properties in the axial direction were defined by using the power law model. This varying in properties leads to complex the vibration behavior and increases the nonlinearity. The impact of modulus ratio, density ratio as well as material distribution parameter on the fundamental frequency and mode shape of simply supported axial-FG beam was investigated.

2. PROBLEM CHARACTERIZATION

The basic idea of FGMs can be summarized as “design the material properties to get on the required static or dynamic response”. Therefore, the material properties (i.e. mechanical and physical properties) are studied essentially in order to understand the behavior of FGMs. Generally, three mathematical equations are widely used to define the mechanical and physical properties of FGMs. These mathematical equations are power-law, sigmoid and exponential equations [35-37]. In this study, the distribution of material in axial direction is defined by "power-law equation". Using the rule of mixture, the mechanical (Modulus of Elasticity and Poison Ratio) and physical (Density) properties of power-law axial-FG beam can be written as (see Figure 1):

$$V_L = \left(1 - \left(\frac{X}{L}\right)\right)^{\beta} \tag{1}$$

$$V_L + V_R = 1 \tag{2}$$

$$\begin{aligned} E(X) &= (E_L * V_L) + (E_R * V_R) \\ &= (E_L - E_R) * \left(1 - \left(\frac{X}{L}\right)\right)^{\beta} + E_R \end{aligned} \tag{3}$$

$$\mu(X) = (\mu_L - \mu_R) * \left(1 - \left(\frac{X}{L}\right)\right)^{\beta} + \mu_R \tag{4}$$

$$\rho(X) = (\rho_L - \rho_R) * \left(1 - \left(\frac{X}{L}\right)\right)^{\beta} + \rho_R \tag{5}$$

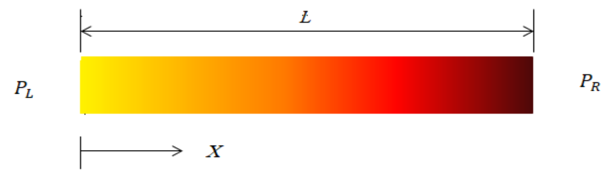

(a) Axial FG-beam

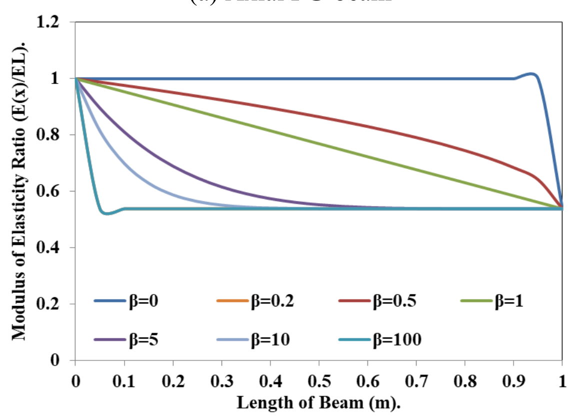

(b) Distribution of modulus ratio

Figure 1. Distribution of properties along the length of axial-FGB

Generally, the stiffness of uniform beam is the main parameters effect on the response of beam and the stiffness equals to the multiplying of elastic modulus and second moment of cross section area of the beam. In axial functionally graded beam (axial-FGB), the elastic modulus is not constant along the axial direction (i.e. non-uniform properties). Due to this non-uniformity in material properties along the axial direction, the classical solutions (depending on Euler beam theory, Timoshenko beam theory and high order shear theory) of free vibration problem are not accurate [36]. Therefore, these theories or solutions must be modified to consider the variation in properties along the length of beam.

3. RAYLEIGH METHOD

The Rayleigh Method is a simple numerical method that used to calculate the natural frequency. This method considers Euler beam theory therefore it is not accurate when it is used for calculating natural frequency of axial-FGB because of varying the material properties along the length of beam (see Eqs. (3)-(5)). In this work, the Rayleigh Method is modified to overcome the varying in material properties. In order to compute the natural frequency and mode shape of axial-FGB with simply supported conditions, the problem of non-uniformity in material properties must solved. In this study, the Rayleigh method (RM) is utilized to solve this problem using homogenization technique [2, 3]. The homogenization technique is applied to find the equivalent stiffness of axial-FGB as illustrated in the following steps [2, 3]:

1. Dividing the beam into (M) parts and (M+1) points and the length of each part is ($\Delta X = L/M$).
2. Calculating mechanical properties (modulus of elasticity and Poisons ratio) and physical property (density) at each point using Eqs. (6)-(8) as illustrated in Figure 2, the position of any point is $X = \Delta X * (i-1); i = 1,2,3, \dots\ M+1$.

$$E(X) = (E_L - E_R) * \left(1 - \left(\frac{\Delta X * (i-1)}{L}\right)\right)^{\beta} + E_R; \quad i = 1,2,3, \dots \dots M+1 \tag{6}$$

$$\mu(X) = (\mu_L - \mu_R) * \left(1 - \left(\frac{\Delta X * (i-1)}{L}\right)\right)^{\beta} + \mu_R; \quad i = 1,2,3, \dots \dots M+1 \tag{7}$$

$$\rho(X) = (\rho_L - \rho_R) * \left(1 - \left(\frac{\Delta X * (i-1)}{L}\right)\right)^{\beta} + \rho_R; \quad i = 1,2,3, \dots \dots M+1 \tag{8}$$

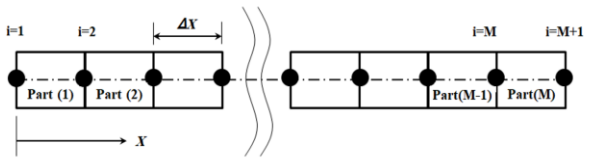

Figure 2. Dividing the axial-FGB

3. Calculating the modulus of elasticity, Poisons ratio and density of each part by taking the average value of start and end points of each part:

$$E(part\ i) = \frac{\left(E(point\ i+1) + E(point\ i)\right)}{2}; \quad i = 1,2,3, \dots \dots M \tag{9}$$

$$\mu(part\ i) = \frac{\left(\mu(point\ i+1) + \mu(point\ i)\right)}{2}; \quad i = 1,2,3, \dots \dots M \tag{10}$$

$$\rho(part\ i) = \frac{\left(\rho(point\ i+1) + \rho(point\ i)\right)}{2}; \quad i = 1,2,3, \dots \dots M \tag{11}$$

4. Calculating the equivalent stiffness of the simply supported axial-FGB by the following steps:

(i) Compute the center of volume of the axial-FGB (X_c) using the following equation:

$$X_c = \frac{\sum_{i=1}^{M} X_i * \mathbb{V}_i}{\sum_{i=1}^{M} \mathbb{V}_i} \tag{12}$$

where, $\mathbb{V}_i$ is the volume of (i) part.

The center of axial-FGB in this case equals (0.5*L) (uniform area).

i. Dividing the beam into two cantilever beams at the position X_c as shown in Figure 3.
ii. Calculating the equivalent stiffness of the two-cantilever axial-FGBs using the following equation:

$$\left((EI)_{eq}\right)_L = \frac{(L_{Left})^3}{\sum_{k=1}^{M_{Left}} \frac{(L_k)^3 - (L_{k-1})^3}{(EI)_k}}; \quad K = 1,2, \dots . M_{Left} \tag{13}$$

$$\left((EI)_{eq}\right)_R = \frac{(L_{Right})^3}{\sum_{k=1}^{M_{Right}} \frac{(L_k)^3 - (L_{k-1})^3}{(EI)_k}}; \quad K = 1,2, \dots . M_{Right} \tag{14}$$

The total equivalent stiffness is:

$$(EI)_{eq} = \frac{(L_{Right} + L_{Left}) * (L_{Right})^2 * (L_{Left})^2}{\left(\left(\sum_{K=1}^{M_{Right}} \frac{{l_{K-1}}^3 - {l_K}^3}{I_K}\right) * {L_{Right}}^2\right) + \left(\left(\sum_{K=1}^{M_{Left}} \frac{{l_K}^3 - {l_{K-1}}^3}{I_K}\right) * {L_{Left}}^2\right)} \tag{15}$$

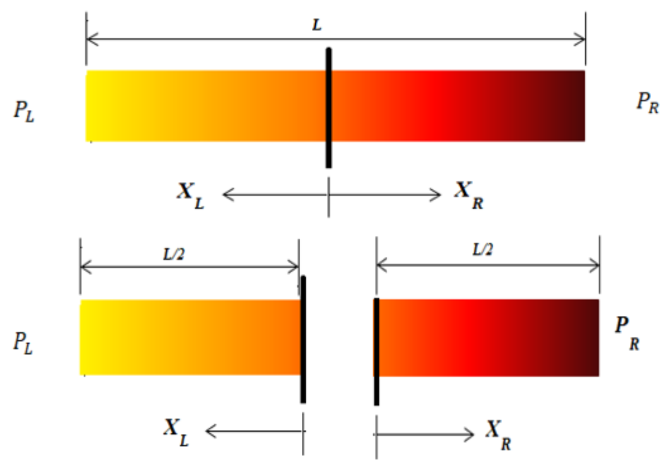

Figure 3. Dividing the simply supported beam into two cantilever beam depending on the centroid of axial-FGB

5. Calculating deflections of simply supported beam by applying the equivalent stiffness and using Table 1 and the equation (considering W=1):

$$[Y] = [\delta][F] \tag{16}$$

where, $[F] = f_i$, $i = 1, 2, 3, \ldots. M + 1$ and it is called "external force matrix" and in the free vibration the values of f_i are calculated as:

$$f_i = \begin{cases} \frac{\rho(part\ 1)*\Delta X*A*g}{2} & \text{when } i = 1 \\ \frac{\rho(part\ M)*\Delta X*A*g}{2} & \text{when } i = M + 1 \\ \rho(part\ i) * \Delta X * A * g & \text{when } i \neq 1 \text{ and } i \neq M + 1 \end{cases} \tag{17}$$

Table 1. Deflection equations of different points in simply supported beam

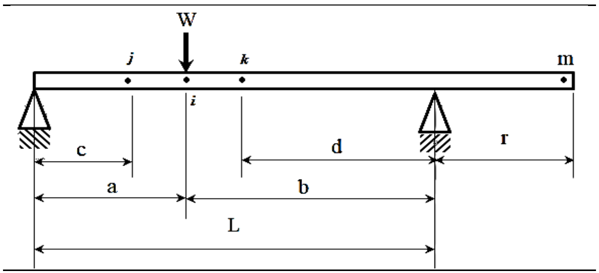

$\delta ji = WbcL^2 - b^2 - c^2 6EIL$

$$\delta_{ii} = \frac{Wa^2b^2}{3EIL}$$

$$\delta_{ki} = \frac{Wad(L^2 - a^2 - d^2)}{6EIL}$$

$$\delta_{mi} = \frac{Wabr(L + a)}{6EIL}$$

6. Applying the boundary conditions of simply supported beam as:

$$\begin{gathered} At\ X = 0 \to f_1 = 0; \delta_{1j} = \delta_{j1} = 0; \\ j = 1,2,3, \ldots. M + 1 \\ At\ X = L \to f_{(M+1)} = 0; \delta_{(M+1)j} = \delta_{j(M+1)} = 0; \\ j = 1,2,3, \ldots. M + 1 \end{gathered} \tag{18}$$

7. Calculating the natural frequency using the following equation:

$$\omega^2 = \frac{g * \sum_{i=1}^{M+1} y_i * f_i}{\sum_{i=1}^{M+1} (y_i)^2 * f_i} \tag{19}$$

4. FINITE ELEMENT MODEL

In this paper, the finite element model is used to calculate the natural frequency and mode shapes of the simply supported axial-FGB. The present finite element model applied the element "BEAM189" using ANSYS APDL software and the "Model Analysis" is adopted in this work. The convergence criteria applied by Wadi et al. [2] is also adopted in this work. The simply supported axial-FGB is divided into (20) parts (i.e. M=20) and each part contains five elements. The properties of element" BEAM189" were summarized in references [2, 3]. The boundary conditions of the simply supported beam are:

(1) At X=0, Ux=Uy=Uz=0.
(2) At X=L, Uy=Uz=0.

These boundary conditions are assumed theoretically to satisfy that "the length of mid plane in simply supported beam remains constant". Also, these boundary conditions were used in several engineering FGM applications.

5. VALIDATION OF THE PRESENT MODELS

For checking the accuracy of Rayleigh and ANSYS models of the present work, the fundamental frequency results of two models are compared with the results obtained by Alshorbagy et al. [15] and Al-Zaini et al. [35]. Mechanical and physical properties of simply supported axial-FGB used by Alshorbagy et al. [15] and Al-Zaini et al. [35] are listed in Table 2. They considered that the steel is the left material and they calculated the properties of right material according to modulus and density ratios (they assumed the density ratio =1). Alshorbagy et al. [15] used axial-FGB with length and width equal to 20m and 0.4m respectively, while the thickness (or height) of axial FGB is calculated with reference to the ratio of length to thickness. Alshorbagy et al. [15] used two values of the length-to- thickness ratio and these values were 20 and 100. Alshorbagy et al. [15] and Al-Zaini et al. [35] used the parameter of the non-dimensional frequency to display this comparison. The parameter of the non-dimensional frequency is written as [15, 35]:

$$\lambda^2 = \omega L^2 \sqrt{\frac{\rho_R}{E_R} \frac{A}{I}} \tag{20}$$

Table 2. The mechanical and physical properties of the materials used for checking accuracy of the present models [15, 35]

Property	Unit	Metal (Steel)	Ceramic (Alumina (Al_2O_3))
Modulus of Elasticity (E)	Pa.	$210.0*10^9$	$390.0*10^9$
Poisson Ratio (μ)	…	0.28	0.33
Density (ρ)	kg/m^3	7800	3960

Table 3. Comparison of the frequency parameters for validation of the present models with different power law index (β), modulus ratio (E_L/E_R) and length-to-height ratio (L/h)

E_L/E_R	Power Law Index (β)	L/h=20				
		Author				
		Present Work		Al-Zaini et al. [35]		Alshorbagy et al. [15]
		Rayleigh Method	ANSYS-BEAM189	ANSYS-SHELL281	ANSYS-SOLID186	
0.25	0.1	2.329939	2.33845	2.3375	2.3394	2.3285
	0.2	2.413451	2.4154	2.4104	2.4204	2.4106
	0.5	2.590268	2.58385	2.5783	2.5894	2.5821
	1	2.767177	2.7529	2.7481	2.7577	2.7533

	2	2.945109	2.9263	2.9221	2.9305	2.9278
	5	3.096288	3.0806	3.0766	3.0846	3.0834
	10	3.133192	3.12455	3.1205	3.1286	3.1265
	0.1	2.688463	2.6891	2.6838	2.6944	2.6868
	0.2	2.727505	2.72805	2.7228	2.7333	2.7258
	0.5	2.817994	2.81635	2.8114	2.8213	2.8148
0.5	1	2.91655	2.91115	2.9065	2.9158	2.9104
	2	3.021393	3.0117	3.0074	3.016	3.0122
	5	3.113747	3.1041	3.0999	3.1083	3.1052
	10	3.136731	3.1308	3.1266	3.135	3.1316
	0.1	3.142715	3.14035	3.136	3.1447	3.14
	0.2	3.142715	3.14035	3.136	3.1447	3.14
	0.5	3.142715	3.14035	3.136	3.1447	3.14
1	1	3.142715	3.14035	3.136	3.1447	3.14
	2	3.142715	3.14035	3.136	3.1447	3.14
	5	3.142715	3.14035	3.136	3.1447	3.14
	10	3.142715	3.14035	3.136	3.1447	3.14
	0.1	3.702872	3.69705	3.6933	3.7008	3.6988
	0.2	3.670116	3.66345	3.6598	3.6671	3.6653
	0.5	3.582165	3.57365	3.57	3.5773	3.5758
2	1	3.467642	3.46025	3.4564	3.4641	3.4611
	2	3.326629	3.3252	3.321	3.3294	3.3244
	5	3.188623	3.20415	3.2095	3.1988	3.1923
	10	3.152372	3.15455	3.1501	3.159	3.1531
	0.1	4.38226	4.37375	4.3702	4.3773	4.3768
	0.2	4.321689	4.31055	4.3073	4.3138	4.3144
	0.5	4.151365	4.1344	4.1314	4.1374	4.1387
4	1	3.911783	3.89045	3.8872	3.8937	3.8937
	2	3.592089	3.58005	3.576	3.5841	3.5795
	5	3.258158	3.26985	3.2653	3.2744	3.2668
	10	3.167217	3.1754	3.1709	3.1799	3.1726

		L/h=100				
E_L/E_R	Power Law Index (β)	Author				
		Present Work		Al-Zaini et al. [35]		Alshorbagy et al. [15]
		Rayleigh Method	ANSYS-BEAM189	ANSYS-SHELL281	ANSYS-SOLID186	
	0.1	2.32994	2.332	2.3336	2.3304	2.3297
	0.2	2.413451	2.4138	2.415	2.4126	2.4118
	0.5	2.590267	2.58455	2.5852	2.5839	2.5834
0.25	1	2.767177	2.7549	2.7552	2.7546	2.7546
	2	2.94511	2.9295	2.9296	2.9294	2.9293
	5	3.096287	3.0844	3.0844	3.0844	3.0849
	10	3.133192	3.1278	3.1278	3.1278	3.1281
	0.1	2.688463	2.69025	2.6914	2.6891	2.6881
	0.2	2.727505	2.7291	2.7301	2.7281	2.7271
	0.5	2.817993	2.8176	2.8182	2.817	2.8162
0.5	1	2.916549	2.91285	2.9131	2.9126	2.9119
	2	3.021392	3.01405	3.0141	3.014	3.0137
	5	3.113747	3.1068	3.1068	3.1068	3.1067
	10	3.13673	3.1334	3.1334	3.1334	3.1332
	0.1	3.142715	3.14235	3.1423	3.1424	3.1415
	0.2	3.142715	3.14235	3.1423	3.1424	3.1415
	0.5	3.142715	3.14235	3.1423	3.1424	3.1415
1	1	3.142715	3.14235	3.1423	3.1424	3.1415
	2	3.142715	3.14235	3.1423	3.1424	3.1415
	5	3.142715	3.14235	3.1423	3.1424	3.1415
	10	3.142715	3.14235	3.1423	3.1424	3.1415
	0.1	3.702873	3.6993	3.6975	3.7011	3.7006
	0.2	3.670115	3.6658	3.664	3.6676	3.6671
	0.5	3.582166	3.5762	3.5746	3.5778	3.5775
2	1	3.467642	3.46275	3.4618	3.4637	3.4628
	2	3.326628	3.3274	3.3272	3.3276	3.326
	5	3.188623	3.1959	3.1959	3.1959	3.1939
	10	3.152373	3.156	3.156	3.156	3.1547
	0.1	4.382258	4.37575	4.3719	4.3796	4.3789
	0.2	4.321688	4.3125	4.3082	4.3168	4.3166
	0.5	4.151364	4.13625	4.1314	4.1411	4.1408
4	1	3.911783	3.89285	3.8894	3.8963	3.8957
	2	3.592089	3.5828	3.582	3.5836	3.5812
	5	3.258157	3.2713	3.2713	3.2713	3.2684
	10	3.167217	3.1765	3.1765	3.1765	3.1742

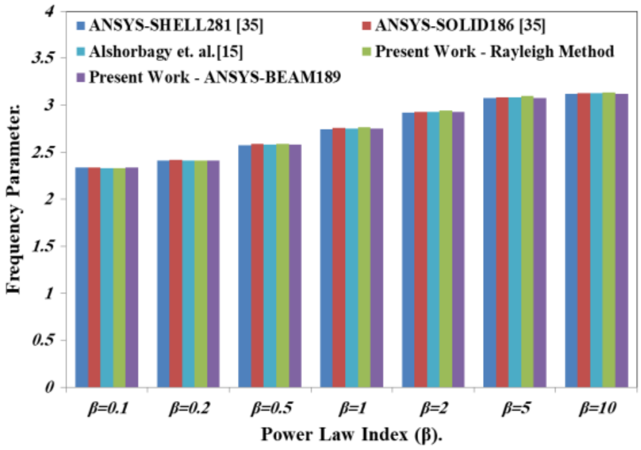

L/h=20.

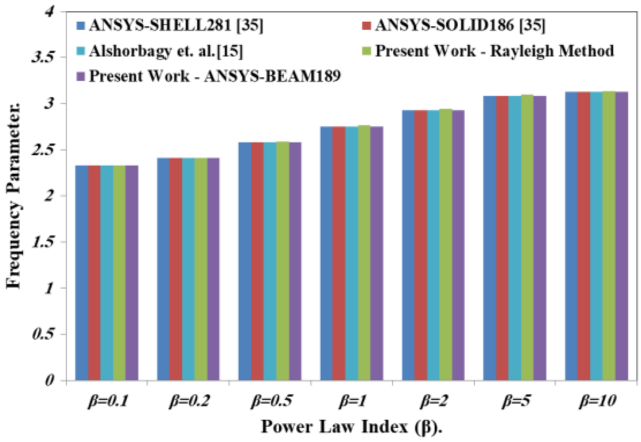

L/h=100.

Modulus Ratio=0.25

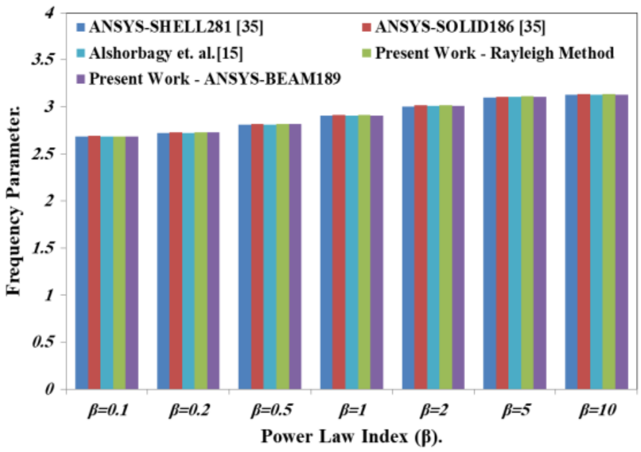

L/h=20.

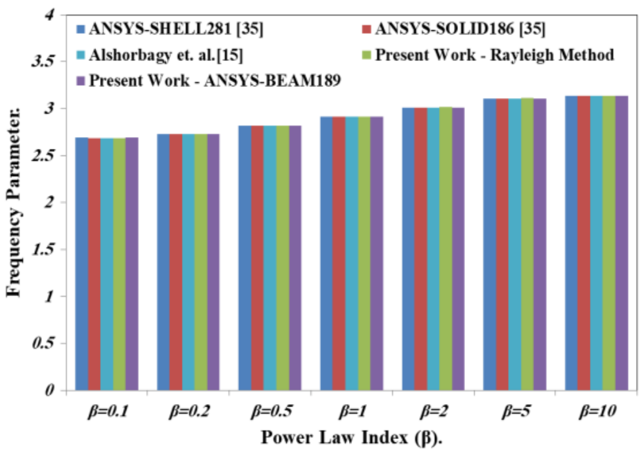

L/h=100.

Modulus Ratio=0.5

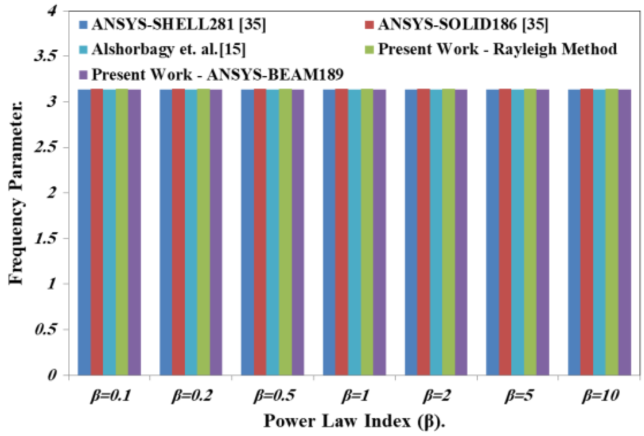

L/h=20.

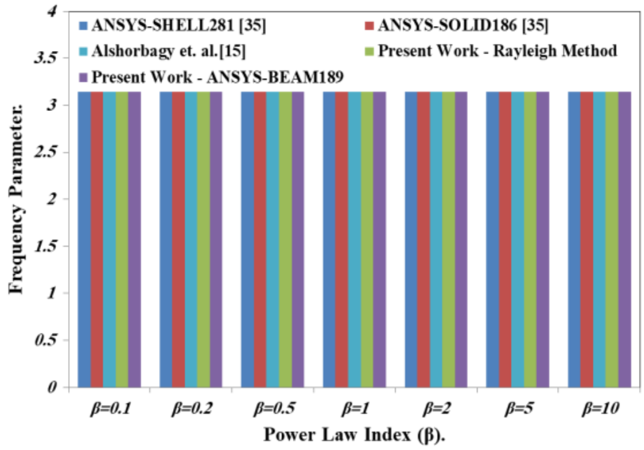

L/h=100.

Modulus Ratio=1

L/h=20.

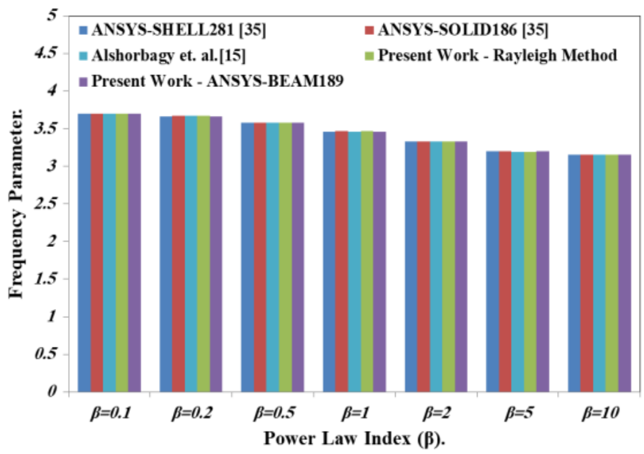

L/h=100.

Modulus Ratio=2

L/h=20.

L/h=100.

Modulus Ratio=4

Figure 4. Comparison of the frequency parameters for validation of the present models with different length-to-height ratio (L/h), modulus ratio (Ec/Em) and power law index (β)

Table 3 and Figure 4 show the comparison of fundamental frequency parameter results of the simply supported axial-FGB estimated by Alshorbagy et al. [15], Al-Zaini et al. [35] (two ANSYS models using SOLID186 and SHELL281) and present models (Rayleigh and ANSYS-BEAM189 models) with various different modulus ratio and power-law index (β). It is noted that an excellent agreement between the present models and the models used by Alshorbagy et al. [15] and Al-Zaini et al. [35] at any modulus ratio and power-law index (β). Also, the length-to-thickness ratio doesn't affect the frequency parameter calculated by Rayleigh model.

6. RESULTS AND DISCUSSION

In this work, steel is chosen as a left material and when the modulus ratio or density ratio change, the material properties of the right material are varied only. The dimensions of axial-FGB are: Length=1m and width=thickness=0.05m. Three important parameters, that effect on the natural frequency and mode shape of axial-FGB, are studied in this paper and these parameters are power-law index (β) (or material distribution parameters), modulus-ratio (E_L/E_R) and density-ratio (ρ_L/ρ_R).

6.1 Fundamental frequency

Figure 5 shows the effect of power-law index (β) on the non-dimensional frequency parameter with various modulus-ratio (E_L/E_R) and the density-ratio (ρ_L/ρ_R) is constant. When (ρ_L/ρ_R=0.25), the non-dimensional frequency parameter reduces with decreasing the power-law index (β) as illustrated in Figure 5(a). The increase of power-law index (β) leads to increase the equivalent stiffness of axial-FGB. The increase in equivalent stiffness causes reducing non-dimensional fundamental frequency parameter. Also, the slop (i.e. rate of variation) of frequency parameter increases with increasing the value of modulus-ratio (E_L/E_R). The slop (i.e. rate of variation) frequency parameter when (E_L/E_R=4) is the largest slop when the power-law index (β) increases. Also, when (E_L/E_R=0.25), the non-dimensional fundamental frequency parameter is approximately constant with increasing power-law index (β) (i.e. the slop (i.e. rate of variation) of frequency parameter is approximately zero). If (ρ_L/ρ_R=1), the non-dimensional fundamental frequency parameter increases with increasing the power-law index (β) when the value of modulus-ratio (E_L/E_R) is smaller than (1). Also, the non-dimensional fundamental frequency parameter decreases with increasing the power-law index (β) when the value of modulus-ratio (E_L/E_R) is larger than (1) (see Figure 5(c)). In Figure 5(e) (ρ_L/ρ_R=4), the non-dimensional fundamental frequency parameter increases with increasing the power-law index (β) when the modulus-ratio (E_L/E_R) is smaller than (4). While the non-dimensional fundamental frequency parameter is approximately constant with increasing the power-law index (β) when (E_L/E_R=4).

In Figure 6, the fundamental frequency of axial-FGB is affected by power-law index (β) with various density-ratio (ρ_L/ρ_R) and the modulus-ratio (E_L/E_R) constant. The fundamental frequency is approximately constant with increasing when the power-law index (β) when density-ratio equals modulus-ratio (i.e. ρ_L/ρ_R=E_L/E_R). According to Eqs. (3) and (5), the summation variation of material properties (modulus and density) gives a constant value of fundamental frequency when the power-law index (β) increases. In other side, when the modulus -ratio is greater than density -ratio (i.e. ρ_L/ρ_R<E_L/E_R), the fundamental frequency reduces with increasing the power-law index (β). And the rate of decreasing of fundamental frequency increases with increasing the power-law index (β) and modulus-ratio. While if the modulus-ratio is smaller than density-ratio (i.e. ρ_L/ρ_R>E_L/E_R), the fundamental frequency increases with increasing the power-law index (β) and the rate of increasing of fundamental frequency increases with increasing the power-law index (β) and decreasing modulus-ratio. This behavior occurs due to combined effects of two important factors (equivalent stiffness and mass distribution of axial-FGB). In Eqs. (3) and (5) and when (ρ_L/ρ_R =E_L/E_R), the elastic modulus and density of axial-FGB varied with the same way when the power-law index (β) increases. The variation in elastic modulus leads to vary the equivalent stiffness of axial-FGB and density along the axial-FGB leads. If the elastic modulus increases, the fundamental frequency increases, while the fundamental frequency decreases when density (i.e. mass distribution) increases. The increasing in fundamental frequency due to increase elastic modulus equals to the decreasing in fundamental frequency due to increase density. Therefore, the fundamental frequency is constant when (ρ_L/ρ_R =E_L/E_R).

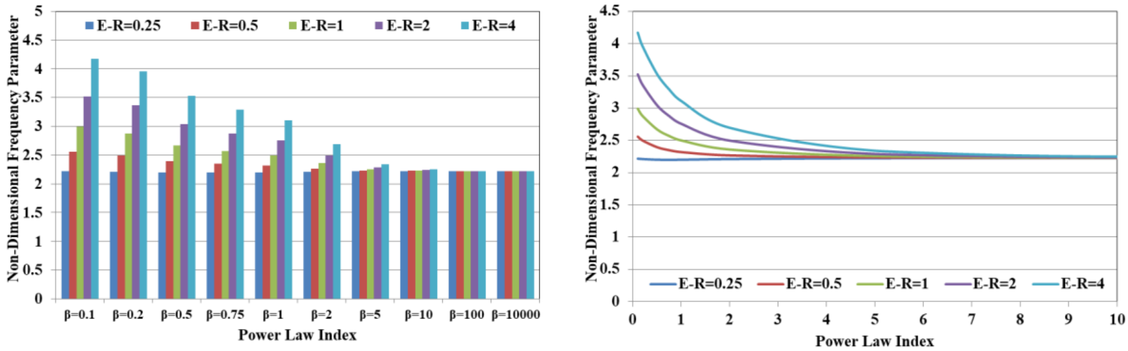

(a) ρ_L/ρ_R=0.25

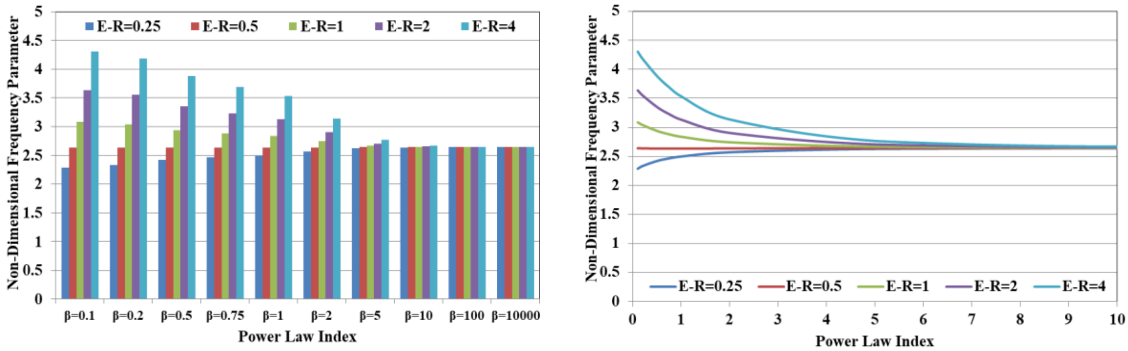

(b) ρ_L/ρ_R=0.5

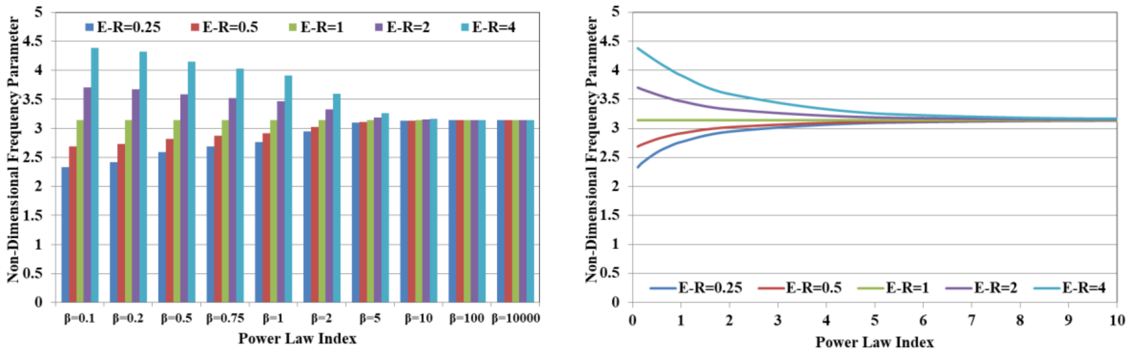

(c) ρ_L/ρ_R=1

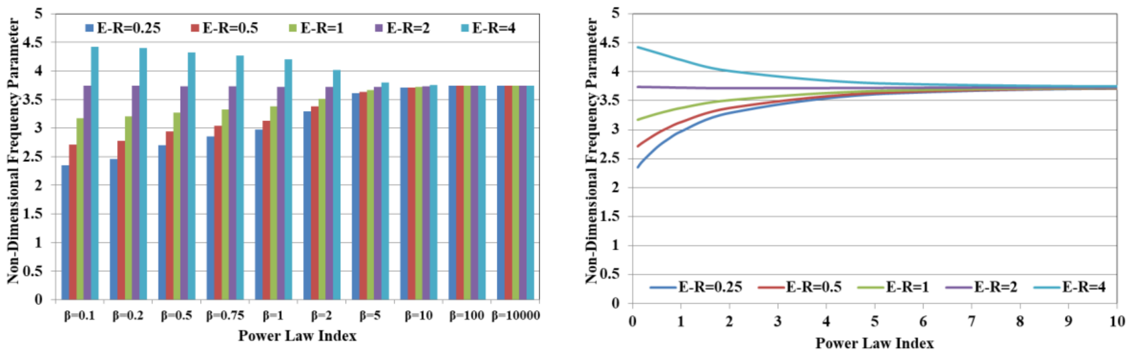

(d) ρ_L/ρ_R=2

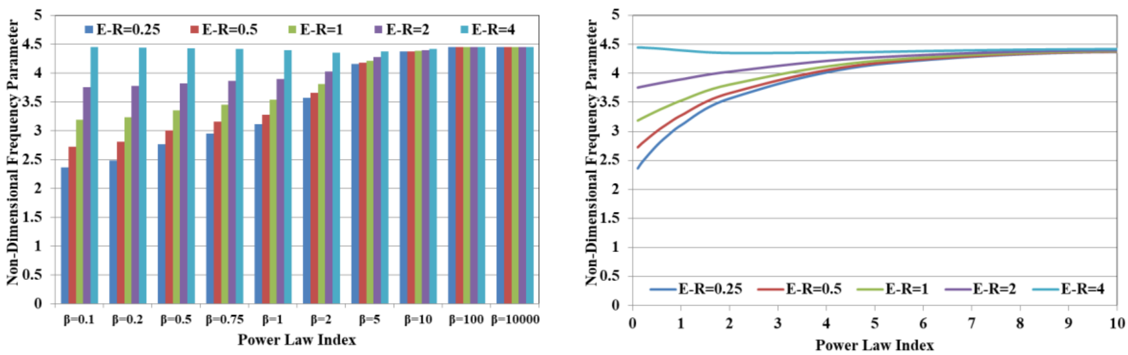

(e) ρ_L/ρ_R=4

Figure 5. Effect of power-law index (β) on the non-dimensional frequency parameters with various modulus and density ratios

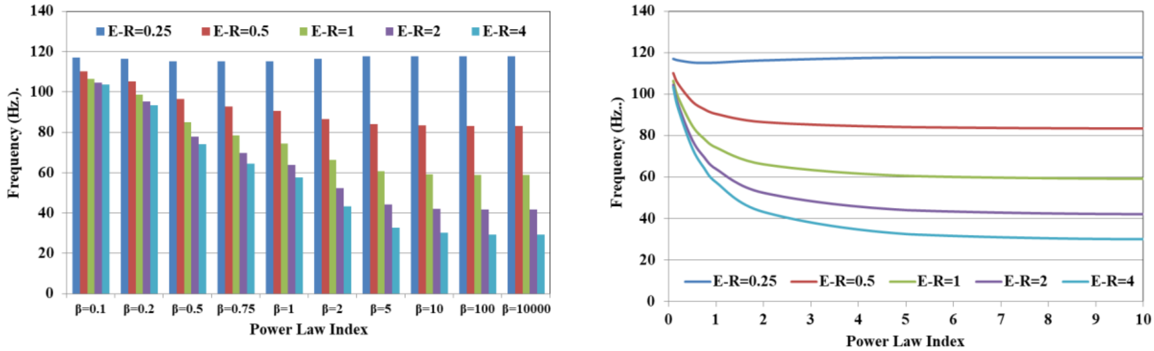

(a) ρ_L/ρ_R=0.25

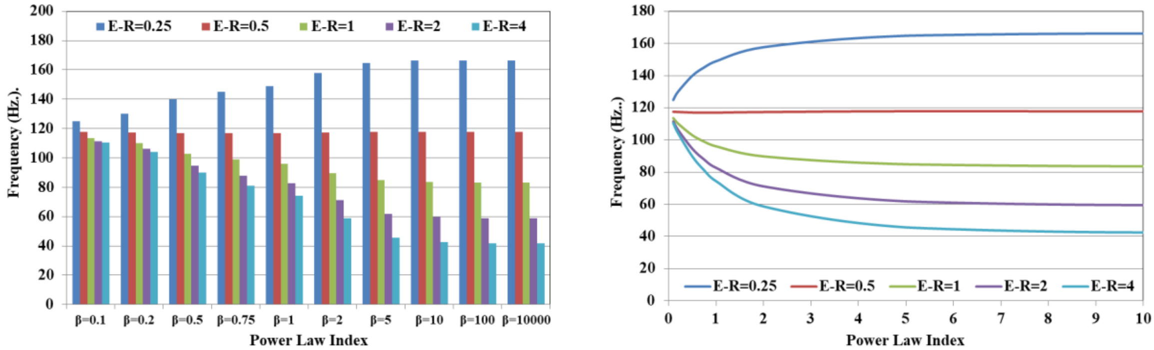

(b) ρ_L/ρ_R=0.5

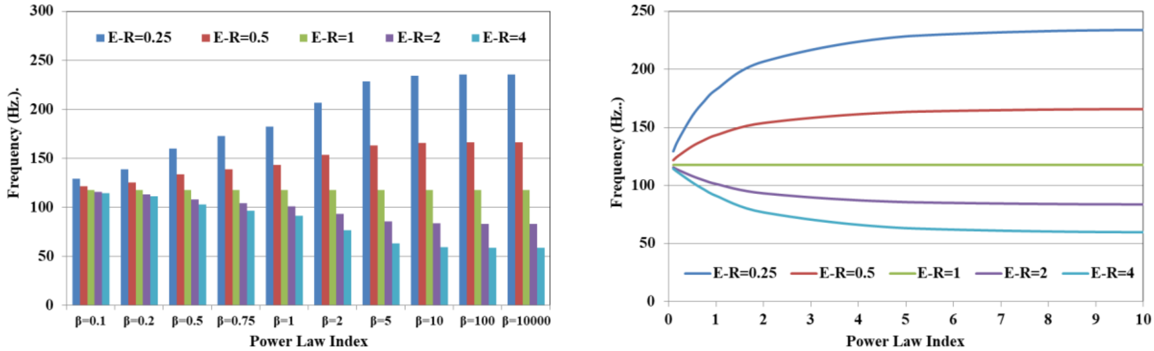

(c) ρ_L/ρ_R =1

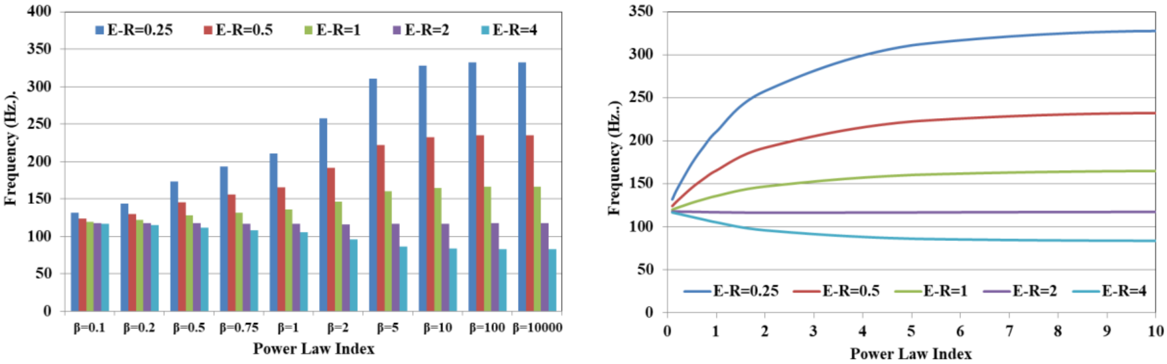

(d) ρ_L/ρ_R =2

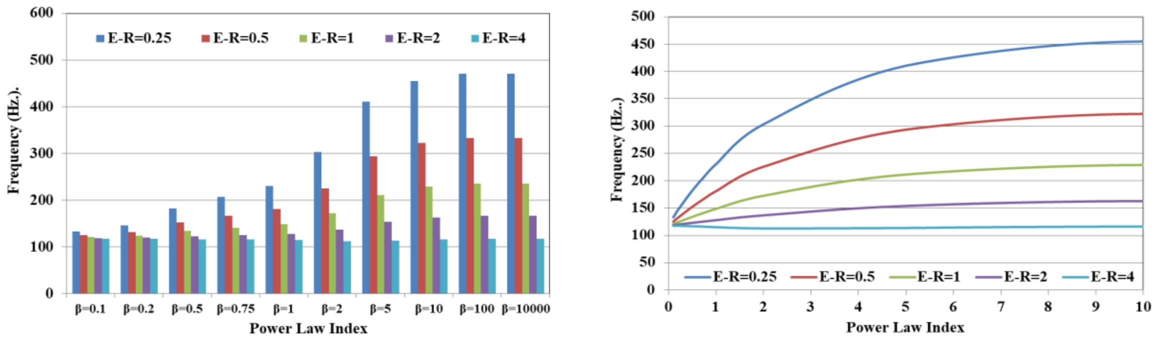

(e) ρ_L/ρ_R=4

Figure 6. Effect of power–law index (β) on fundamental frequency with various modulus and density ratios

Finally, Figure 7 displays the combination effects of modulus and density ratios on the non-dimensional frequency parameter with various power-law index (β). When (β=1) (i.e. linear variation), the effect of density-ratio (**ρ_L/ρ_R**) is similar to the effect of modulus-ratio (**E_L/E_R**). It is clear that the maximum non-dimensional frequency parameter occurs when (**ρ_L/ρ_R=E_L/E_R**=4) and the minimum non-dimensional frequency parameter occurs when (**ρ_L/ρ_R =E_L/E_R**=0.25). For (β<1), the effect of modulus-ratio (**E_L/E_R**) is greater than that of density-ratio (**ρ_L/ρ_R**). While the effect of modulus-ratio (**E_L/E_R**) is smaller than that of density-ratio (**ρ_L/ρ_R**) when (β>1).

From the results, the combination effects of modulus ratio, density ratio and power law index are described and illustrated. Practically, the FGM beam is used is several engineering applications and some of these applications requires vibration criteria. Therefore, the designer of FGM beam can used the data in Figures 5-7 to select the suitable parents of FGM by choosing the modulus-ratio and density ratio.

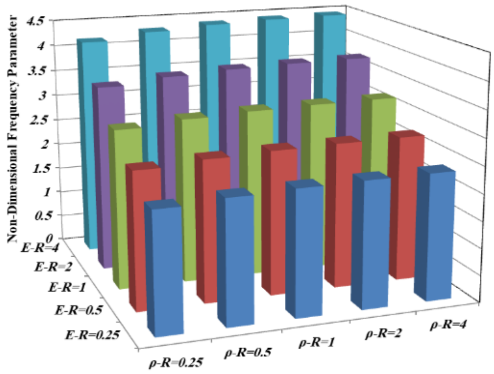

β=0.1

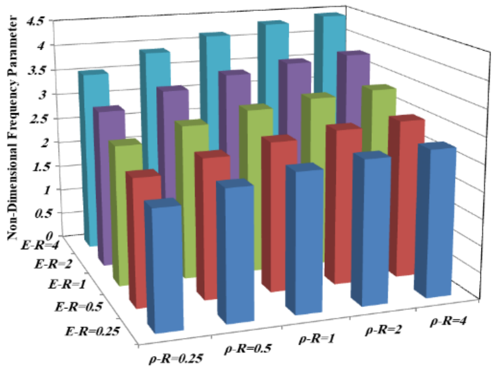

β=0.5

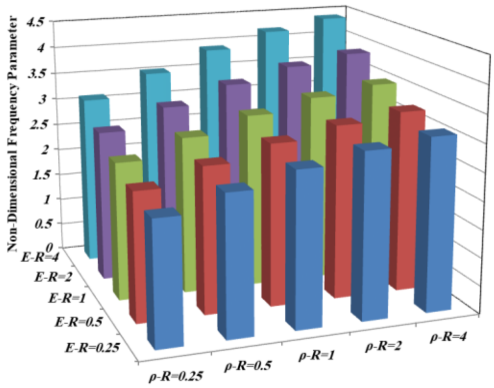

β=1

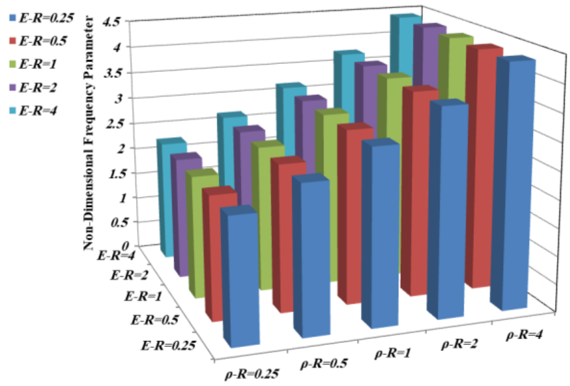

β=5

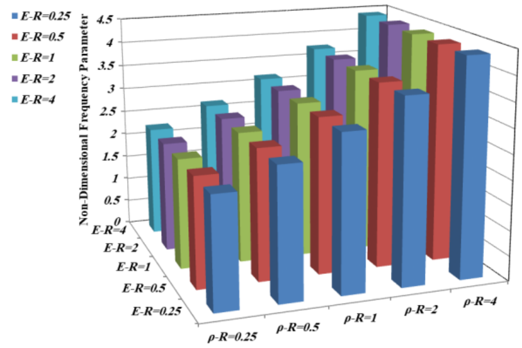

β=10

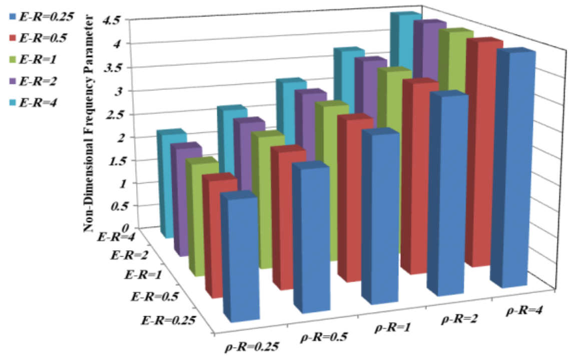

β=10000

Figure 7. Effect of power–law index (β), modulus ratio and density ratio on fundamental frequency with various

6.2 Mode shape

The effects of power-law index (β), modulus-ratio (**E_L/E_R**) and density-ratio (**ρ_L/ρ_R**) on the mode shapes of axial-FGBs illustrate in Figures 8-12. When (**ρ_L/ρ_R**=0.25), the effect of power-law index (β) on mode shape increases with increasing modulus-ratio (**E_L/E_R**) as shown in Figure 8. When the power-law index (β) increases, the dimensionless deflection (or amplitude) increases too. In other side, the effect of power-law index (β) on mode shape increases with reducing modulus-ratio (**E_L/E_R**) when (**ρ_L/ρ_R**=4) as shown in Figure 12 and the dimensionless deflection (or amplitude) increases with reducing power-law index (β). If (**ρ_L/ρ_R**=1), the effect of power-law index (β) on mode shape appeases sharply at the maximum and minimum modulus-ratio (**E_L/E_R**) (i.e. **E_L/E_R**=4 and **E_L/E_R**=0.25) as illustrated in Figure 10. Also, the dimensionless deflection (or amplitude) increases with reducing the power-law index (β) when (***E$_L$/E$_R$***<1), and increases with increment of the power-law index (β) at (***E$_L$/E$_R$***>1).

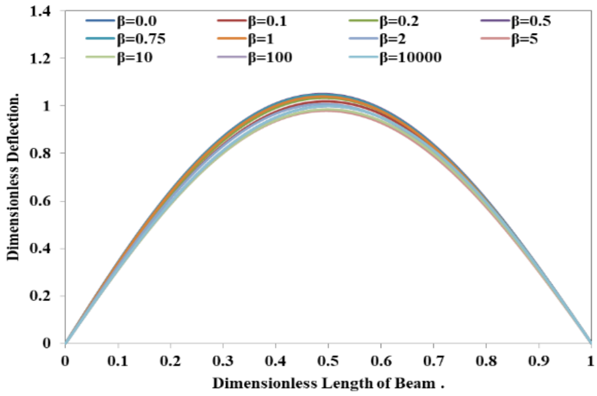

$E_L/E_R=0.25$

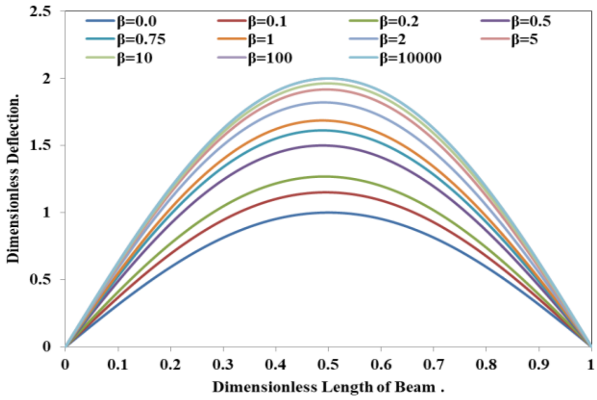

$E_L/E_R=0.5$

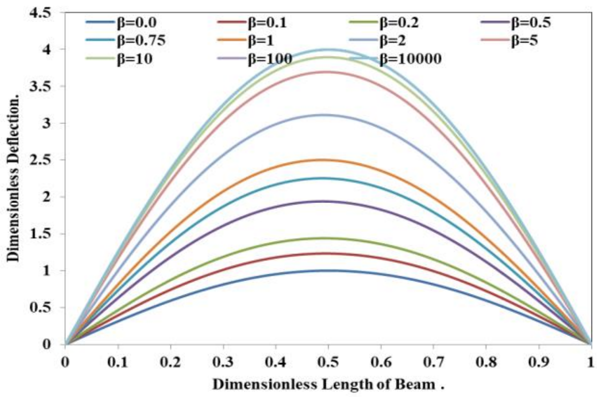

$E_L/E_R=1$

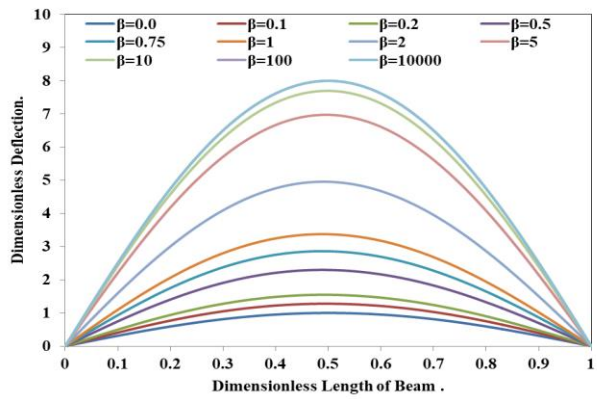

$E_L/E_R=2$

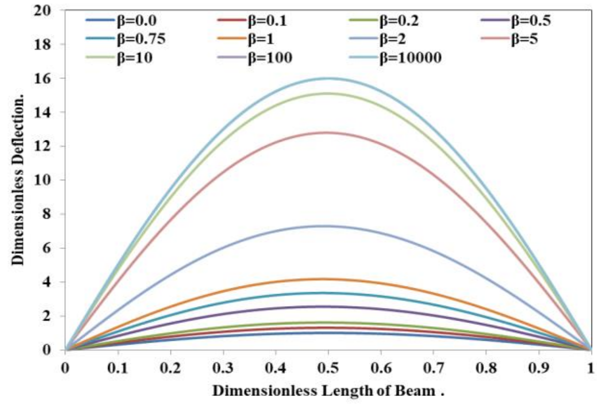

$E_L/E_R=4$

Figure 8. Effect of power-law index (β) and modulus ratio on the non-dimensional mode shape when the density ratio=0.25

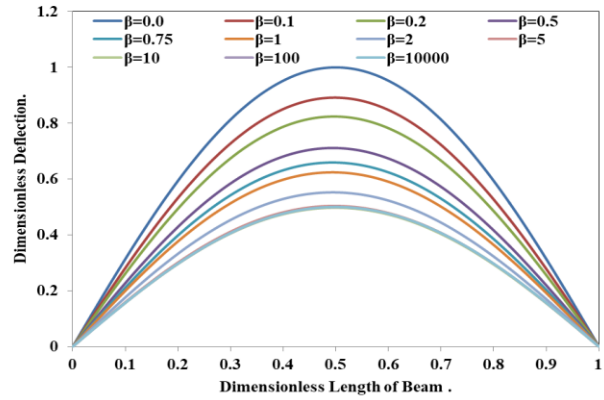

$E_L/E_R=0.25$

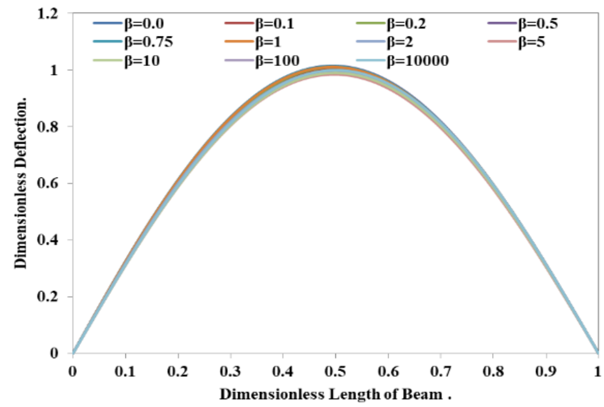

$E_L/E_R=0.5$

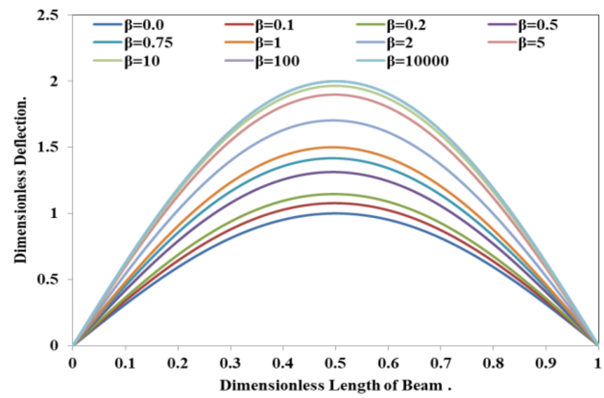

$E_L/E_R=1$

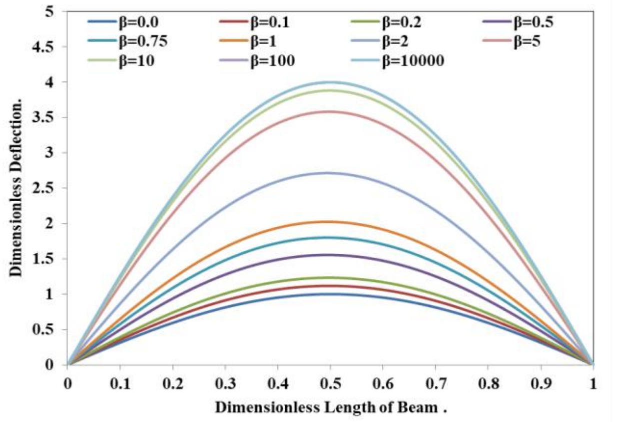

$E_L/E_R=2$

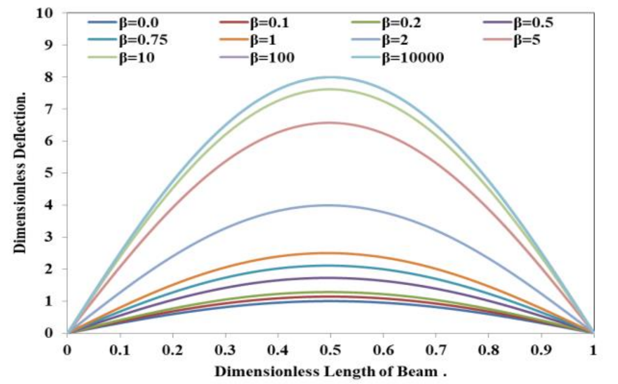

$E_L/E_R=4$

Figure 9. Effect of power-law index (β) and modulus ratio on the non-dimensional mode shape when the density ratio=0.5

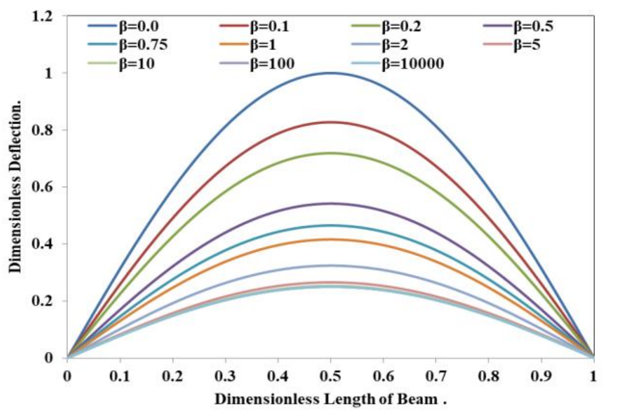

$E_L/E_R=0.25$

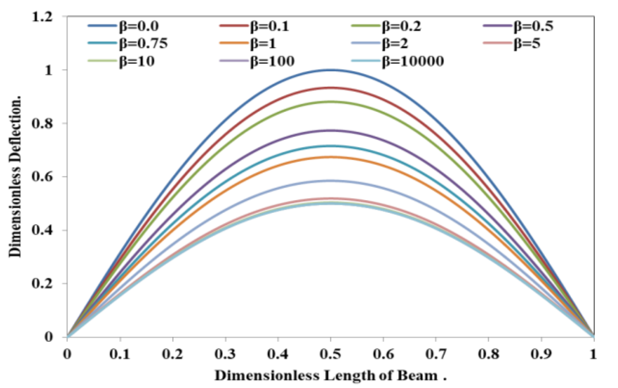

$E_L/E_R=0.5$

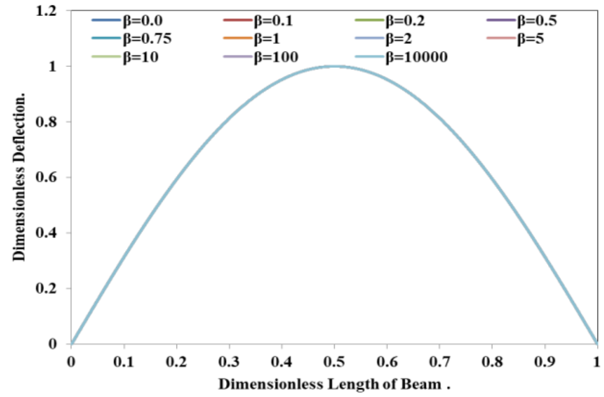

$E_L/E_R=1$

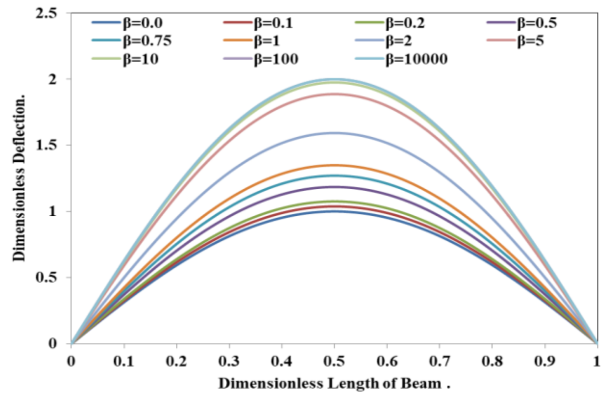

$E_L/E_R=2$

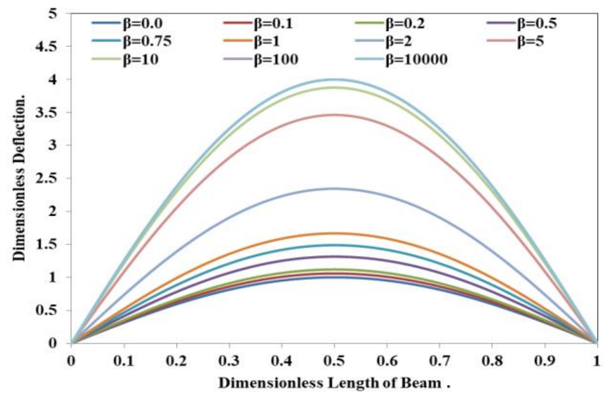

$E_L/E_R=4$

Figure 10. Effect of power-law index (β) and modulus ratio on the non-dimensional mode shape when the density ratio=1

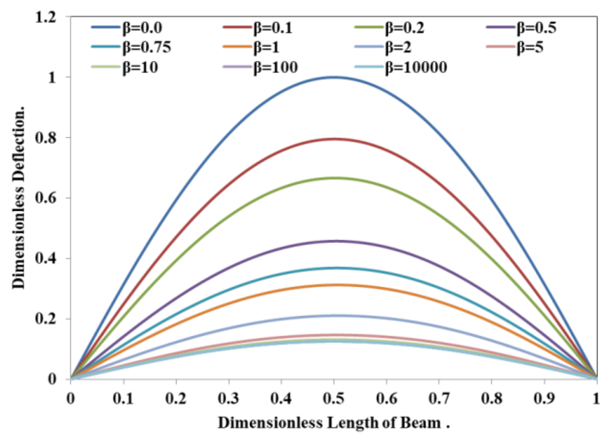

$E_L/E_R=0.25$

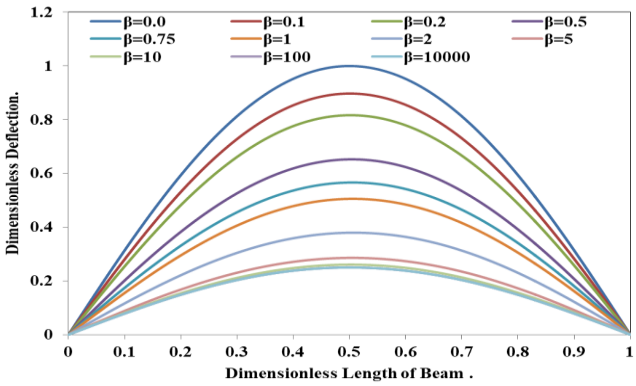

E_L/E_R=0.5

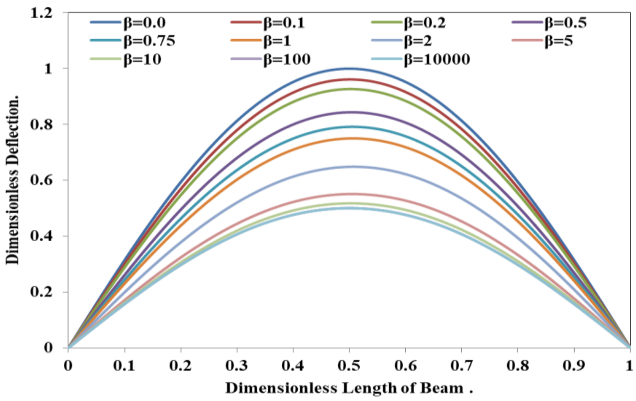

E_L/E_R=1

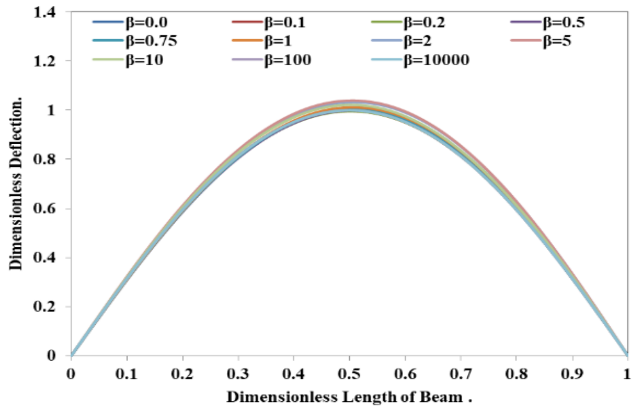

E_L/E_R=2

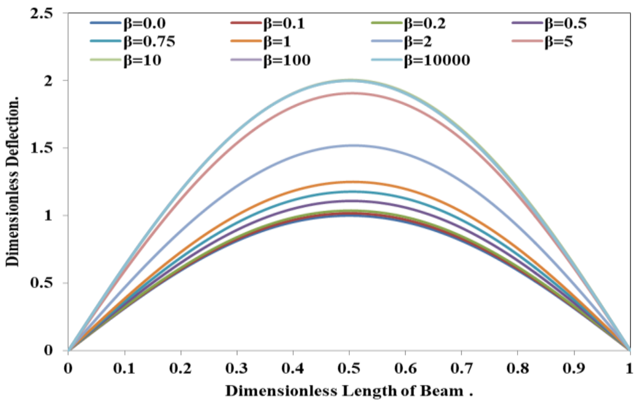

E_L/E_R=4

Figure 11. Effect of power-law index (β) and modulus ratio on the non-dimensional mode shape when the density ratio=2

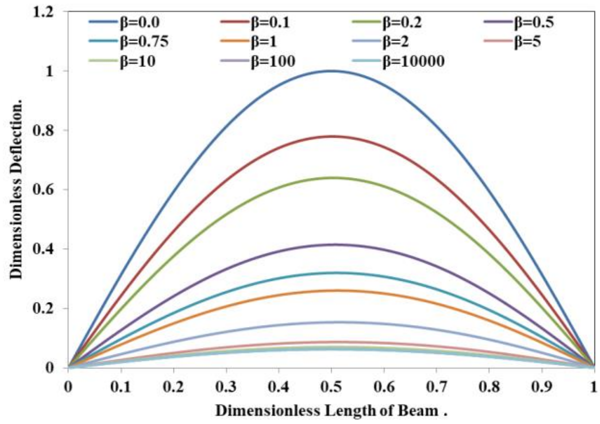

E_L/E_R=0.25

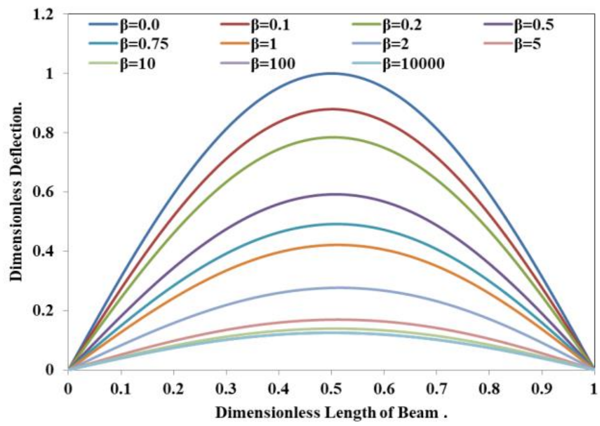

E_L/E_R=0.5

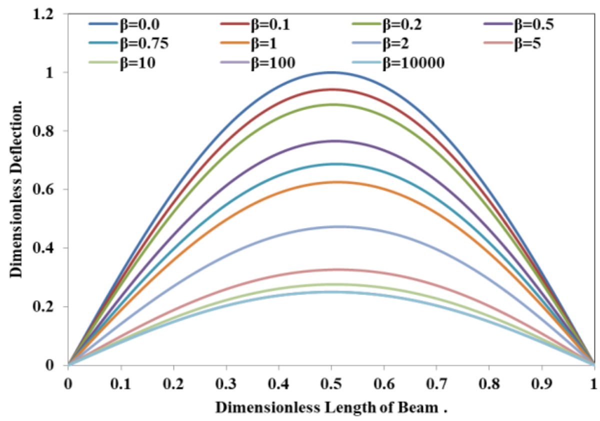

E_L/E_R=1

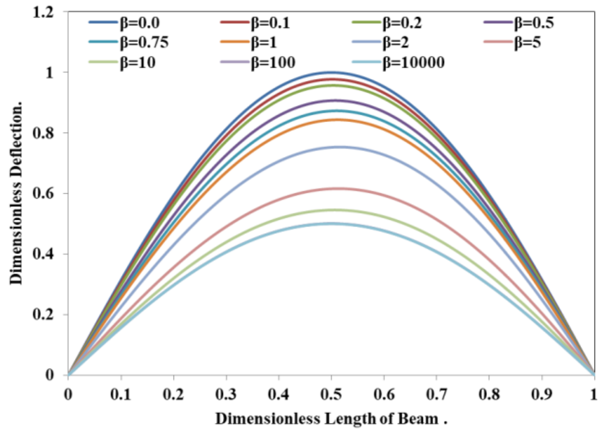

E_L/E_R=2

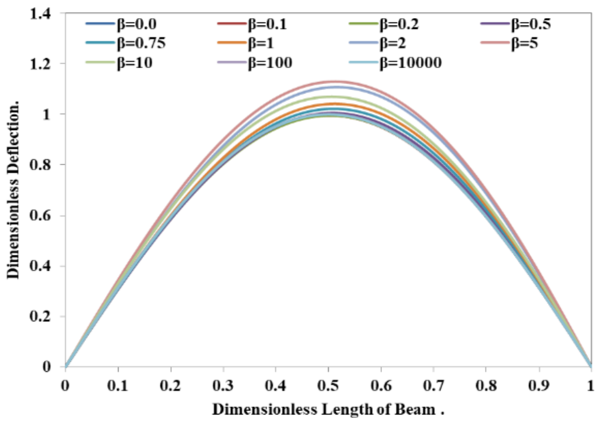

E_L/E_R=4

Figure 12. Effect of power–law index (β) and modulus ratio on the non-dimensional mode shape when the density ratio=4

7. CONCLUSIONS AND FUTURE WORKS

In this paper, the Rayleigh method was adopted to simulate the free vibration problem of simply supported axial-FGB. The main purpose of this study is to investigate the combined effects of power-law index, (β), modulus-ratio (E_L/E_R) and density-ratio (ρ_L/ρ_R) on the fundamental frequency and mode shapes of axial-FGBs and that is reached by results. From the results discussed in previous section, the following points can be concluded.

1) For fundamental frequency parameter, non-dimensional fundamental frequency parameter is approximately constant with increment of power-law index (β) at modulus-ratio equals to density-ratio (i.e. $E_L/E_R = \rho_L/\rho_R$).
2) For fundamental frequency parameter, the non-dimensional fundamental frequency parameter increases with increasing the power-law index (β) when the value of modulus-ratio (E_L/E_R) is smaller than (1) and decreases with increasing the power-law index (β) when the value of modulus-ratio (E_L/E_R) is larger than (1) when (ρ_L/ρ_R=1).
3) For fundamental frequency parameter, if (β=1) (i.e. linear variation), the effect of density-ratio (ρ_L/ρ_R) on the fundamental frequency parameter is similar to the effect of modulus-ratio (E_L/E_R). It is clear that the maximum and minimum non-dimensional frequency parameter occurs when ($\rho_L/\rho_R = E_L/E_R$=4) and ($\rho_L/\rho_R=E_L/E_R$=0.25) respectively.
4) For fundamental frequency parameter, when (β<1), the effect of modulus-ratio (E_L/E_R) is greater than that of density-ratio (ρ_L/ρ_R). While the effect of modulus-ratio (E_L/E_R) is smaller than that of density-ratio (ρ_L/ρ_R) when (β>1).
5) For mode shape, when (ρ_L/ρ_R=1) the dimensionless deflection (or amplitude) increases with reducing the power-law index (β) at (E_L/E_R<1), and it increases with increment the power-law index (β) at (E_L/E_R>1).

For future works, the combination effects of modulus-ratio (E_L/E_R), power-law index (β) and density-ratio (ρ_L/ρ_R) on the natural frequencies and mode shapes of second and third modes for axial-FGBs under different boundary conditions can be investigated using Rayleigh and finite element methods.

REFERENCES

[1] Saleh, B., Jiang, J., Fathi, R., Al-Hababi, T., Xu, Q., Wang, L., Song, D., Ma, A. (2020). 30 Years of functionally graded materials: An overview of manufacturing methods, applications and future challenges. Composites Part B: Engineering, 201: 108376. https://doi.org/10.1016/j.compositesb.2020.108376

[2] Wadi, K.J., Yadeem, J.M., Al-Ansari, L.S., Abdulsamad, H.J. (2022). Static deflection calculation for axially FG cantilever beam under uniformly distributed and transverse tip loads. Results in Engineering, 14: 100395. https://doi.org/10.1016/j.rineng.2022.100395

[3] Hashim, W.M., Alansari, L.S., Aljanabi, M., Raheem, H.M. (2022). Investigating static deflection of non-prismatic axially functionally graded beam. Material Design & Processing Communications, 2022(1): 7436024. https://doi.org/10.1155/2022/7436024

[4] Shukur, Z.M., Hamad, R.F., Ali, Y.K., Al-Ansari, L.S., Al-Karaishi, M.H. (2023). Investigating the effect of applying uniform distributed load on the deflection of simply supported axial - functionally graded beam. Journal of Aerospace Technology and Management, 15: e2423. https://doi.org/10.1590/jatm.v15.1315

[5] Mahamood, R.M., Akinlabi, E.T., Shukla, M., Pityana, S.L. (2012). Functionally graded material: An overview. In Proceedings of the World Congress on Engineering 2012 Vol III (WCE 2012), London, UK.

[6] Ebhota, W.S., Jen, T.C. (2018). Casting and applications of functionally graded metal matrix composites. Advanced Casting Technologies, 59.

[7] Li, Y., Feng, Z., Hao, L., Huang, L., Xin, C., Wang, Y., Bilotti, E., Essa, K., Zhang, H., Li, Z., Yan, F., Peijs, T. (2020). A review on functionally graded materials and structures via additive manufacturing: From multi-scale design to versatile functional properties. Advanced Materials Technologies, 5(6): 1900981. https://doi.org/10.1002/admt.201900981

[8] Beldjelili, Y., Tounsi, A., Mahmoud, S.R. (2016). Hygro-thermo-mechanical bending of S-FGM plates resting on variable elastic foundations using a four-variable trigonometric plate theory. Smart Structures and Systems, An International Journal, 18(4): 755-786. https://doi.org/10.12989/sss.2016.18.4.755

[9] Vatanabe, S.L., Rubio, W.M., Silva, E.C.N. (2014), Modeling of Functionally Graded Materials. In Comprehensive Materials Processing, pp. 261-282. https://doi.org/10.1016/B978-0-08-096532-1.00222-3

[10] Shabana, Y.M., Noda, N., Tohgo, K. (2000). Elasto-plastic thermal stresses in functionally graded materials considering microstructure effects. In Current Advances in Mechanical Design and Production VII. Pergamon, pp. 223-231. https://doi.org/10.1016/B978-008043711-8/50023-4

[11] Bouafia, K., Kaci, A., Houari, M.S.A., Benzair, A., Tounsi, A. (2017). A nonlocal quasi-3D theory for bending and free flexural vibration behaviors of functionally graded nanobeams. Smart Structures and Systems, 19(2): 115-126. https://doi.org/10.12989/sss.2017.19.2.115

[12] Elishakoff, I., Guede, Z. (2004). Analytical polynomial solutions for vibrating axially graded beams. Mechanics of Advanced Materials and Structures, 11(6): 517-533. https://doi.org/10.1080/15376490490452669

[13] Çalım, F.F. (2009). Free and forced vibrations of non-uniform composite beams. Composite Structures, 88(3): 413-423. https://doi.org/10.1016/j.compstruct.2008.05.001

[14] Huang, Y., Li, X.F. (2010). A new approach for free vibration of axially functionally graded beams with non-uniform cross-section. Journal of Sound and Vibration, 329(11): 2291-2303. https://doi.org/10.1016/j.jsv.2009.12.029

[15] Alshorbagy, A.E., Eltaher, M.A., Mahmoud, F. (2011). Free vibration characteristics of a functionally graded beam by finite element method. Applied Mathematical Modelling, 35(1): 412-425. https://doi.org/10.1016/j.apm.2010.07.006

[16] Shahba, A., Attarnejad, R., Hajilar, S. (2011). Free vibration and stability of axially functionally graded tapered Euler-Bernoulli beams. Shock and Vibration, 18(5): 683-696. https://doi.org/10.3233/sav-2010-0589

[17] Shahba, A., Attarnejad, R., Marvi, M.T., Hajilar, S. (2011). Free vibration and stability analysis of axially functionally graded tapered Timoshenko beams with classical and non-classical boundary conditions. Composites Part B: Engineering, 42(4): 801-808. https://doi.org/10.1016/j.compositesb.2011.01.017

[18] Shahba, A., Rajasekaran, S. (2012). Free vibration and stability of tapered Euler-Bernoulli beams made of axially functionally graded materials. Applied Mathematical Modelling, 36(7): 3094-3111. https://doi.org/10.1016/j.apm.2011.09.073

[19] Hein, H., Feklistova, L. (2011). Free vibrations of non-uniform and axially functionally graded beams using Haar wavelets. Engineering Structures, 33(12): 3696-3701. https://doi.org/10.1016/j.engstruct.2011.08.006

[20] Huang, Y., Yang, L.E., Luo, Q.Z. (2013). Free vibration of axially functionally graded Timoshenko beams with non-uniform cross-section. Composites Part B: Engineering, 45(1): 1493-1498. https://doi.org/10.1016/j.compositesb.2012.09.015

[21] Akgöz, B., Civalek, Ö. (2013). Free vibration analysis of axially functionally graded tapered Bernoulli-Euler microbeams based on the modified couple stress theory. Composite Structures, 98: 314-322. https://doi.org/10.1016/j.compstruct.2012.11.020

[22] Li, X.F., Kang, Y.A., Wu, J.X. (2013). Exact frequency equations of free vibration of exponentially functionally graded beams. Applied Acoustics, 74(3): 413-420. https://doi.org/10.1016/j.apacoust.2012.08.003

[23] Tang, A.Y., Wu, J.X., Li, X.F., Lee, K.Y. (2014). Exact frequency equations of free vibration of exponentially non-uniform functionally graded Timoshenko beams. International Journal of Mechanical Sciences, 89: 1-11. https://doi.org/10.1016/j.ijmecsci.2014.08.017

[24] Sarkar, K., Ganguli, R. (2014). Closed-form solutions for axially functionally graded Timoshenko beams having uniform cross-section and fixed-fixed boundary condition. Composites Part B: Engineering, 58: 361-370. https://doi.org/10.1016/j.compositesb.2013.10.077

[25] Garijo, D. (2015). Free vibration analysis of non-uniform Euler-Bernoulli beams by means of Bernstein pseudospectral collocation. Engineering with Computers, 31(4): 813-823. https://doi.org/10.1007/s00366-015-0401-6

[26] Zhao, Y., Huang, Y., Guo, M. (2017). A novel approach for free vibration of axially functionally graded beams with non-uniform cross-section based on Chebyshev polynomials theory. Composite Structures, 168: 277-284. https://doi.org/10.1016/j.compstruct.2017.02.012

[27] Liu, P., Lin, K., Liu, H., Qin, R. (2016). Free transverse vibration analysis of axially functionally graded tapered Euler-Bernoulli beams through spline finite point method. Shock and Vibration, 2016(1): 5891030. https://doi.org/10.1155/2016/5891030

[28] Xie, X., Zheng, H., Zou, X. (2017). An integrated spectral collocation approach for the static and free vibration analyses of axially functionally graded nonuniform beams. Proceedings of the Institution of Mechanical Engineers, Part C: Journal of Mechanical Engineering Science, 231(13): 2459-2471. https://doi.org/10.1177/0954406216634393

[29] Kukla, S., Rychlewska, J. (2016). An approach to free vibration analysis of axially graded beams. Journal of Theoretical and Applied Mechanics, 54. http://doi.org/10.15632/jtam-pl.54.3.859

[30] Huang, Y., Rong, H.W. (2017). Free vibration of axially inhomogeneous beams that are made of functionally graded materials. International Journal of Acoustics and Vibration, 22(1): 68-73. https://doi.org/10.20855/ijav.2017.22.1452

[31] Cao, D., Wang, B., Hu, W., Gao, Y. (2019). Free vibration of axially functionally graded beam. Mechanics of Functionally Graded Materials and Structures. http://doi.org/10.5772/intechopen.85835

[32] Fogang, V. (2021). Vibration analysis of axially functionally graded non-Prismatic Timoshenko beams using the finite difference method. Preprints 2021: 2021050442. https://doi.org/10.20944/preprints202105.0442.v1

[33] Kılıç, B., Özdemir, Ö. (2021). Vibration and stability analyses of functionally graded beams. Archive of Mechanical Engineering, 68. http://doi.org/10.24425/ame.2021.137043

[34] Selmi, A. (2020). Dynamic behavior of axially functionally graded simply supported beams. Smart Structures and Systems, 25(6): 669-678. https://doi.org/10.12989/sss.2020.25.6.669

[35] Al-Zaini, E.O.A., Abboud, Z., Al-Ansari, L.S. (2022). Studying the thermal effects on the free vibration of functionally graded beam. SAE International Journal of Materials and Manufacturing, 15(3): 229-252. https://doi.org/10.4271/05-15-03-0016

[36] Rao, S.S. (2007). Vibration of Continuous Systems. John Wiley & Sons, New York, USA, vol. 464.

[37] ANSYS Mechanical APDL Element Reference, ANSYS, Inc., 2016, https://www.mm.bme.hu/~gyebro/files/vem/ansys_14_element_reference.pdf.

NOMENCLATURES

A	Cross Section Area, m^2
$E(X)$	Modulus of Elasticity at any point (X), Pa
E_L, E_R	Modulus of Elasticity of Left and Right Material, Pa

$[F]$	Force Matrix, N
f_i	Applied Load of Each Point (i), N
$\boldsymbol{I}$	Second Moment of Area, m^4
$\boldsymbol{g}$	Gravitational Acceleration, m/sec^2
$\boldsymbol{L}$	Length of Beam, m
L_{Left}, L_{Right}	Length of the Left and Right Cantilever Beams, m
$\boldsymbol{M}$	Number of Dividing Parts
M_{Left}, M_{Right}	Number of Dividing Parts of the Left and Right Cantilever Beams
Ux, Uy, Uz	Displacement in x, y and z direction, m
V_L, V_R	Volume Fraction of Left and Right Material
$\mathbb{V}_i$	Volume of (i) part, m^3
$\boldsymbol{W}$	Applied Load, N
$\boldsymbol{X}$	Coordinate
$\boldsymbol{X_c}$	Centroid of the Axial FGB, m
$[Y]$	Deflection Matrix, m
β	Power Law Index
$[\delta]$	Delta Matrix, m/N
λ	The Non-dimensional Frequency Parameter
$\mu(X)$	Poison Ratio at any point (X)
μ_L, μ_R	Poison Ratio of Left and Right Material
$\rho(X)$	Density at any point (X), kg/m^3
ρ_L, ρ_R	Density of Left and Right Material, kg/m^3
ω	Frequency, rad/sec